THE JOURNAL OF COMPARATIVE NEUROLOGY 227:540-557 (1984)

The Architecture and Some of the Interconnections of the Rat's Amygdala and Lateral Periallocortex

BLAIR H. TURNER AND JENS ZIMMER
Department of Anatomy, Howard University Medical School, Washington, DC 20059 (B.H.T.); Institute of Anatomy B., University of Aarhus, DK-8000 Aarhus C, Denmark (J.Z.)

ABSTRACT

The connections between the cerebral cortex and amygdala were studied in the rat by means of silver degeneration techniques. To help define the sites of origin and termination of cortico-amygdaloid connections, the architecture of the cortex and the amygdala was studied in sections from normal brains stained for cells, fibers, acetylcholinesterase activity, and heavy metals (Timm staining).

The amygdalopetal cortex on the dorsal and lateral surfaces of the rat brain is limited to a narrow strip of periallocortex that forms the dorsal wall and lip of the rhinal sulcus. Histochemical stains indicate that this cortex comprises several stages of cortical differentiation that are intermediate between the ventrally adjacent allocortices and the dorsally adjacent neocortices. The lateral periallocortex consists of two major divisions, the agranular insula (area 13) anteriorly, and a temporal agranular cortex (areas 35 and 36) posteriorly. The principal amygdaloid target for this cortex is the lateral nucleus. Anterior area 13 and posterior area 35 project to the anterior and posterior halves, respectively, of the medial division of this nucleus, while posterior area 13 and anterior area 35 projects to the lateral division of this nucleus. All divisions of periallocortex also send projections to a part of the putamen that surrounds the lateral half of the central nucleus. All of area 13 also sends efferents to the anterior part of the basal nucleus, while the anterior half of area 13 sends an additional projection to the central nucleus.

Comparison of these data with those obtained in the cat and monkey suggests that a constant feature of eutherian brains is the existence of a subset of efferents from each of the four neocortical sensory systems that is routed so as to provide subcortical limbic structures with modality-specific information. The initial sequence in this sensorilimbic system consists of one or more modality-specific corticocortical relays that originate in the primary sensory cortices and terminate in one of four topographically adjacent, modality-specific areas of the insular and temporal cortices. These insular and temporal areas then each establish modality-specific connections within the amygdaloid complex. The final set of relays presumably comprises the connection that each of these amygdaloid areas makes with the autonomic and endocrine nuclei of the brain.

Key words: histochemistry, limbic, anatomy, connections, phylogeny

Anatomical experiments in the monkey have established that a circumscribed portion of the cortex posterior to the central sulcus sends projections to the amygdaloid complex. These cortical areas comprise the several architectonic divisions of the anterior insula and anterior half of the temporal lobe. Analysis of the distribution of these amygdaloid

Accepted March 21, 1984.

afferents suggested that each architectonic division of cortex was associated with a unique pattern of termination within the amygdala (Turner et al., '80). The present experiments were undertaken in the rat in order to provide a phylogenetic comparison of the sources and projection patterns of cortico-amygdaloid connections. Specifically, we intended to identify which divisons of the rat's neocortex project to the amygdala and to compare their distribution within this structure.

In the course of this study, it became apparent that the sites of origin and termination of the cortical and amygdaloid connections did not always coincide with commonly used architectonic divisions of the cortex and amygdala (Krieg '46; Brodal, '47). Since such discrepancies could have resulted from difficulties encountered in making topographical distinctions based solely on cell or fiber stains, we felt it necessary to the interpretation of our experimental results to reinvestigate the cortical and amygdaloid areas of interest by using heavy metal (Timm) and acetylcholinestinerase (AChE) stains. These results have been reported in summary form (Turner and Zimmer, '80).

MATERIALS AND METHODS

The description of the normal cortical and amygdaloid structures that are reported in the Results is based on series of adjacent, alternately stained sections of brains of eight male rats (Wistar strain) weighing between 150–200 g. Four of these rats were perfused through the heart with a phosphate buffer containing 0.15% sodium sulphide (Haug, '73). The brains were rapidly removed, placed vertically on a microtome stage, and frozen with gaseous carbon dioxide. Brains were cut in a cryostat at 30 μm, thawed onto glass slides, and air dried. Two of the brains were cut in the frontal plane, and the remaining two in the sagittal and horizontal planes. Six parallel series were made of each brain. Two series were stained for AChE activity (Geneser-Jensen and Blackstad, '71) and two were processed by the Timm sulfide silver method (Haug, '73). The final two series were stained for cells and fibers (Hess and Merker, '83). The remaining four rats were perfused, and their brains were processed for catecholamine histofluorescence (Loren et al., '80). Two of these brains were cut frontally, one sagittally, and one horizontally.

Cortical anterograde experiments

In preliminary experiments, four rats with identical cortical lesions were allowed to survive 18 hours, 30 hours, 4 days, or 6 days, and their brains processed by the Fink-Heimer method (Fink and Heimer, '67). Terminal degeneration was seen at all times except after 18 hours, and the extent and density of the terminal degeneration did not vary significantly between 30 hours and six days.

The cortico-amygdaloid results are based upon the brains of 25 male rats (Wistar strain, weighing 150–350 g) that had lesions of the cortical gray matter that did not invade the subjacent white matter. Lesions were made by applying a piece of hot wire briefly onto the cortical surface. Some lesions were intentionally large, but most were 1–2 mm in diameter (Figs. 27, 28). Architectonic classification of lesion sites was made both by fitting dorsal and lateral photographs of experimental brains to cortical maps (Krieg, '46; Turner and Zimmer, '80), and by histological analysis of stained sections through the lesion. At least two cases from each of the major cortical architectonic divisions were available for analysis. The animals survived 3 days, and then were perfused transcardially and their brains cut in a cryostat at 30 μm. Four of the 25 experimental rats were perfused with a sulfide solution, and their brains were stained for cells, fibers, AChE activity, heavy metals (Timm staining), and for anterograde degeneration by Hjorth-Simonsen's ('70) modification of the Fink-Heimer method. Ten rats were perfused with neutralized 4% formaldehyde solution, and the brains were processed by a modification of the Fink-Heimer stain (Tanaka, '76) that permits visualization of cell bodies as well as degeneration. The final 11 rats were perfused for the cupric-silver technique (Olmos, '81). Parallel series of these latter brains were also processed by Hjorth-Simonsen's method, since the cupric-silver stain gives an argyrophilic staining of the central amygdaloid nucleus and closely adjacent areas, which can obscure projections of these regions. For purposes of scanning the sections for terminal fields, it was found desirable to bleach briefly some of the silver-stained sections in 0.5% potassium ferricyanide. When observed under low-power darkfield conditions, the degenerating elements in these sections appear as bright particles. In this viewing condition, the extent and intensity of degeneration are easily seen.

RESULTS

Periallocortical architecture

The cortex that is histologically transitional between six-layered neocortex and one- or two-layered allocortex is designated periallocortex. The cingulate and retrosplenial cortices together form a strip of periallocortex on the medial surface of the brain. A lateral strip of periallocortex lies within and adjacent to the rhinal sulcus, and is the cortex studied in this paper. There are three major subdivisions of this cortex, areas 13a, 13p, and 35 (Fig. 7). In the living animal, the approximate border between areas 13a and 13p is the middle cerebral artery (Fig. 8, *right arrow*) and the approximate border between areas 13p and 35 is shallow, convex deflection of the rhinal sulcus (Fig. 8, *left arrow*). Each area has several subdivisions. The cytoarchitecture of area 13 has been described recently by Krettek and Price ('77a).

Area 13a. In AChE-stained sections (Fig. 2), the outer third of layer I of area 13ad is heavily stained, while the remaining portion of the layer is mildly positive. Layer II is more heavily stained, and layer III less so. A layer IV cannot be identified with certainty. Layers V and VI are moderate in staining intensity with the suggestion of a sublamina in layer VI. The AChE pattern of area 13av is similar to that of area 13ad, except that no sublamina can be discerned in layer VI.

In Timm-stained sections (Fig. 3), layer I of 13ad is dark brown, and layer II is even more intensely stained. Deep to this is a narrow tan layer III. Layer V is again very dark in Timm stains, while layer VI is tan. Layer I of 13av in Timm stained sections can be divided into the sublaminae Ia and Ib that are characteristic of piriform cortex. However, the staining intensity is intermediate between piriform cortex and the cortex of area 13ad. Layers II through V of area 13av are similar to those of area 13ad except that they are thicker, and layer III is traversed by thin, dark filamentous elements that appear to connect layers II and V. Layer VI contains sublaminae consisting of alternating light and dark bans. Areas 13ad and 13av can both be seen in fiber stains (Fig. 1).

Area 13p. The staining patterns of area 13a continue caudally along the rhinal sulcus, although the definition of the laminae becomes less clear (Figs. 1, 4). Areas 13pd and 13pv form the upper and lower lips of the middle third of the rhinal sulcus. Layers I, V, and VI of area 13pd display a moderate staining intensity for AChE (Fig. 5) while layers II and III are faintly stained. With the Timm method (Fig. 6), the outer half of layer I of area 13pd is a moderate brown and the inner half of the layer is a deep gray-brown in appearance. Layers II and V are a deep red-brown separated by a light brown layer II. Layer VI is a uniform tan. In area 13pv, layer III in both AChE and Timm stains disappears, and layers II and V coalesce into a single layer. There is a very narrow, reddish brown layer VI in Timm stains. In cell stains all layers except IV can be distinguished in area 13pd. This cell staining pattern is still visible in area 13pv, although layers V and VI become extremely narrow.

Area 35. Areas 35d and 35v occupy the dorsal and ventral lips of the caudal third of the rhinal sulcus. Layer I of area 35d is moderately stained by the AChE method; further lamination is not apparent except for a very narrow layer VI. Layer I is lightly stained in area 35v, and no other layers are distinguishable. The Timm technique reveals that layer I of area 35d can be divided into a moderately stained outer half and a heavily stained inner half. Layers II and V, which are separated by a tan layer III in the more dorsal cortex of area 36, have coalesced into a single deep brown layer in area 35d. A very narrow layer VI is present. The single layer II/V becomes extremely narrow in area 35v, and a layer VI is absent, being replaced by a staining pattern typical of the deep layers of the piriform-entorhinal transition area. In cell stains of area 35d, narrow layers II, III, and V are discernible, and layer VI is represented by only a few cells. Area 35v is represented by layers II and V.

Architectonic description of the deep amygdaloid nuclei

Since several investigators have described the cytoarchitectonics of the rat amygdala (Brodal, '47; Uchida, '50; Krettek and Price, '78), the following description emphasizes the histochemical architecture of this structure. However, determinations of nuclear boundaries were based also on adjacent cell and fiber stains. Our characterization is limited to the deep nuclei, since it is these that are connected most extensively with the cortex above the rhinal fissure.

The *lateral nucleus* consists of two divisions which, for the most part, are coextensive (Figs. 9–25). The lateral division, AL_1 is bordered laterally by the external capsule and medially by the intermediate capsule. In the anterior half of the amygdala and a narrow extension of this division projects ventrally alongside the anterior division of the basal nucleus. It consists of medium-sized oval and pyramidal cells that are of moderate to deep staining intensity, and are tightly packed. AL_1 is strongly positive for AChE and moderately reactive in Timm staining (Figs. 15, 16). AL_2 is situated medial to AL_1, and at posterior levels is partially encapsulated by it. The cells of this division are also oval or pyramidal in shape, and of medium size. In contrast to AL_1, they are lightly stained and loosely packed. AL_2 displays a light AChE staining but appears deep brown in the Timm method (Figs. 19, 20). Very few catecholamine-containing axons can be observed in either division of the lateral nucleus.

The *basal nucleus* is composed of five divisions (Figs. 9–25). The anterior division, AB_1, is oval in shape and consists of very loosely packed and deeply stained cells. It is intensely stained for AChE and moderately reactive in the Timm method (Figs. 11, 12). AB_2 is located just medial to the ventral tip of the external capsule (Fig. 10) and is present throughout the amygdala except at extreme caudal levels. It is lightly reactive for AChE and dark brown in Timm's stains (Figs. 11, 12). AB_3 and AB_4 (Figs. 21–24) are immediately posterior of AB_1. AB_3 is situated laterally and is made up of medium-sized cells that are moderately stained and packed. In the histochemical methods, this nucleus can be subdivided into lateral (AB_3'') and medial (AB_3') parts. AB_3' is intensely reactive in the AChE method and deep brown in Timm's stains, while AB_3'' is slightly

Abbreviations

a	anterior
AB_1	basal nucleus of the amygdala, anterior part
AB_2	basal nucleus of the amygdala, ventral part
AB_3	basal nucleus of the amygdala, middle part
AB_3'	basal nucleus of the amygdala, middle part, medial division
AB_3''	basal nucleus of the amygdala, middle part, lateral division
AB_4	basal nucleus of the amygdala, medial part
AB_5	basal nucleus of the amygdala, posterior part
ACe	central nucleus of the amygdala
ACO_1	cortical nucleus of the amygdala, anterior part
ACO_2	cortical nucleus of the amygdala, posterolateral part
ACO_3	cortical nucleus of the amygdala, posteromedial part
AHA	hippocampal area of the amygdala
AL_1	lateral nucleus of the amygdala, dorsolateral part
AL_2	lateral nucleus of the amygdala, ventromedial part
AM_1	medial nucleus of the amygdala, anterior part
AM_2'	medial nucleus of the amygdala, posterior part, dorsal division
AM_2''	medial nucleus of the amygdala, posterior part, ventral division
AP_1	putamen area of the amygdala
AP_2	pallidal area of the amygdala
B	bregma
CP	caudoputamen
d	dorsal
E	entorhinal cortex
En	endopiriform nucleus (claustrum)
G	primary gustatory cortex
GP	globus pallidus
H	hippocampus
I	intercalated cells of the amygdala
IA	interaural line
l	lateral
LH	lateral hypothalamus
m	medial
NA	nucleus of the ansa lenticularis
NAOT	nucleus of the accessory olfactory tract
NLOT	nucleus of the lateral olfactory tract
NST(A)	amygdaloid portion of the nucleus of the stria terminalis
p	posterior
Pi	piriform cortex
SII	second somatosensory cortex
TR	transitional cortex
V	lateral ventricle
v	ventral

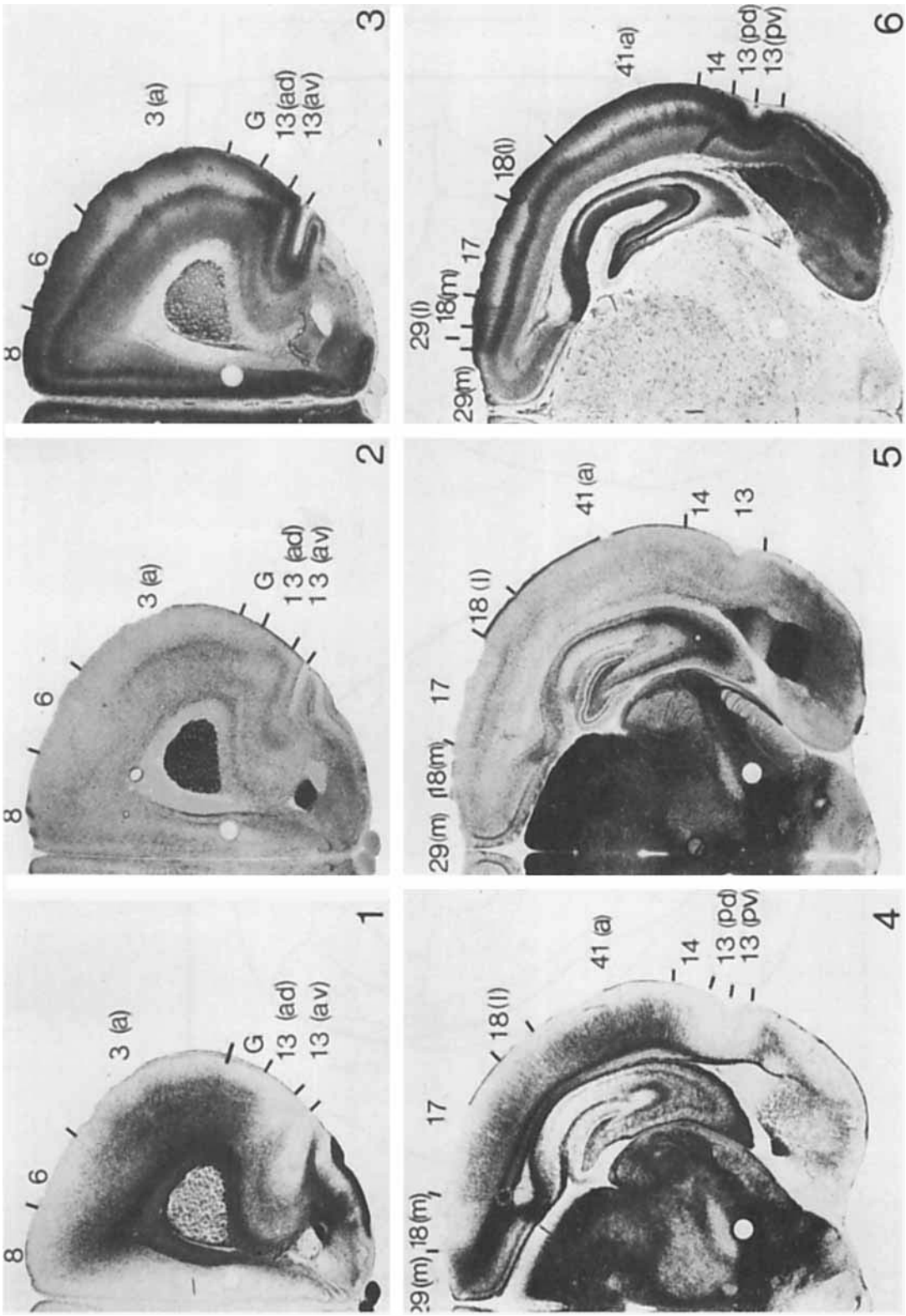

Figs. 1–6. Cortical architectonics in fiber-, AChE-, and Timm-stained material. The boundaries of the cortical areas that are visible in each section are indicated by small black lines, with the designations of the areas placed in between. These sections were taken from the series used for the construction of the cortical maps in Figure 7, where the anteroposterior location of the two levels shown are indicated by vertical lines between the diagrams. Figures 1–3 are adjacent sections at an *anterior* level, while Figures 4–6 are adjacent sections taken more *posteriorly*. Note that the discrimination between areas 18M and 29L can be seen only in the Timm staining (Fig. 6). Burr holes, made in order to keep successive sections in register, can be seen in each section. ×6.2

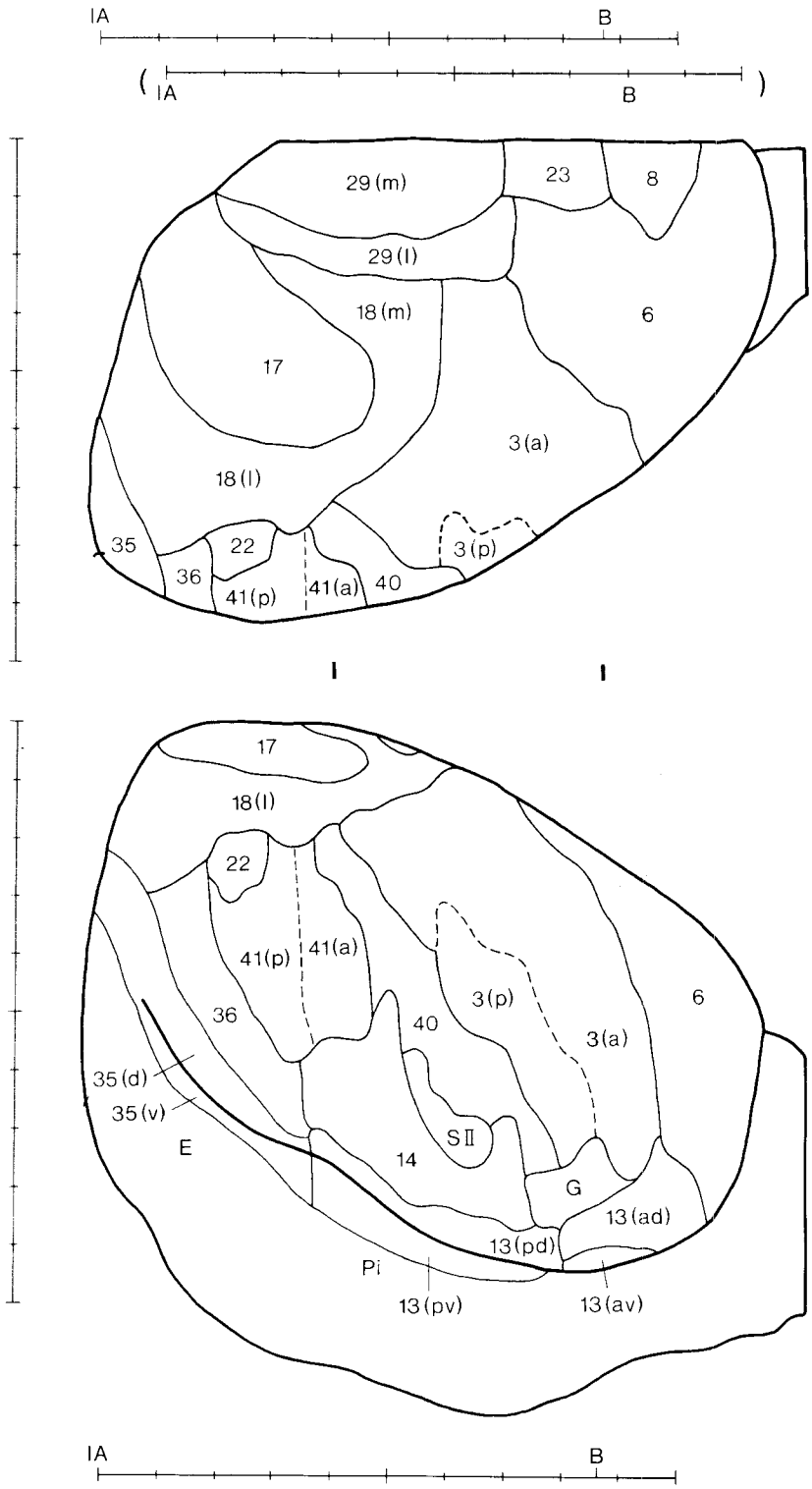

Fig. 7. Dorsal (*top*) and lateral (*bottom*) orthographic reconstructions of the architectonic areas of the cerebral cortex. The architectonic areas are delimited with thin, solid lines. The subdivisions of areas 3 and 41 are drawn with dashed lines. Thick lines are used to define the edges of the brain and the rhinal sulcus. Scales are drawn in millimeters, and the locations of the interaural plane (IA) and the bregma (B) are indicated. In the dorsal projection (top) the anterior parts have undergone foreshortening due to the angle at which the brain was cut. This angle of 22° is apparent in the lateral projection (bottom). Measurements on the dorsal projection can be made as if the dorsal surface of the brain were horizontal by using the scale in parenthesis. The two vertical lines between the diagrams indicate the location of the sections shown in Figures 1–3 and Figures 4–6, respectively.

less reactive for AChE, but more positive in Timm staining. AB_4 is located medially to AB_3, and consists of fairly densely packed, medium-sized, lightly stained cells (Figs. 21–24). The nucleus stains with moderate intensity for both AChE and Timm. The posterior pole of the basal nucleus (AB_5, not illustrated) is made up of medium-sized cells that are loosely packed and deeply stained. The nucleus is very dark in the Timm's stain and moderately reactive for AChE. All basal nuclei receive a moderate catecholamine innervation.

The *accessory basal* nucleus is present in the anterior half of the amygdala (Figs. 9–16, 25) and lies deep to the anterior cortical nucleus (ACo_1). In comparison with ACo_1, the cells of ABA are less densely packed, more lightly stained, and are not organized into laminae. ABA is more lightly stained than ACo_1 by the Timm method.

The *central nucleus*, which is round or ovoid in shape, is present in the anterior half of the amygdala (Figs. 9–16, 25). It is composed of densely packed, moderately stained, round cells that are small to medium in size. The nucleus is almost entirely devoid of AChE activity (Figs. 11, 15), appears yellowish brown in Timm staining, and is densely innervated by catecholamine axons. No subdivisions are apparent, but there are two topographically related structures that together form a shell around the central nucleus. The medial of these (AP_2) is a region that is composed of loosely packed, medium sized, deeply stained cells. The area appears grayish brown in the AChE stain, purple brown in Timm staining, and has a moderate number of catecholamine fibers. The lateral half of the shell appears to be a ventral extension into the amygdala of the putamen (AP_1). This region contains medium-sized, loosely packed, lightly stained cells. In both AChE and Timm stains it is deep brown.

The amygdaloid portion of the *nucleus of the stria terminalis* is situated in the middle third of the amygdala (Figs. 17–20, 25). It consists of densely packed clumps of small, round cells surrounded by a cell-sparse, fibrous area. The region stains lightly for AChE, and light reddish brown with the Timms method.

Cortical areas that do not project to the amygdala

Lesions were made in all of the neocortical areas. None of these areas produced evidence of direct projections to the amygdala (Fig. 26A,B). When these areas are classified

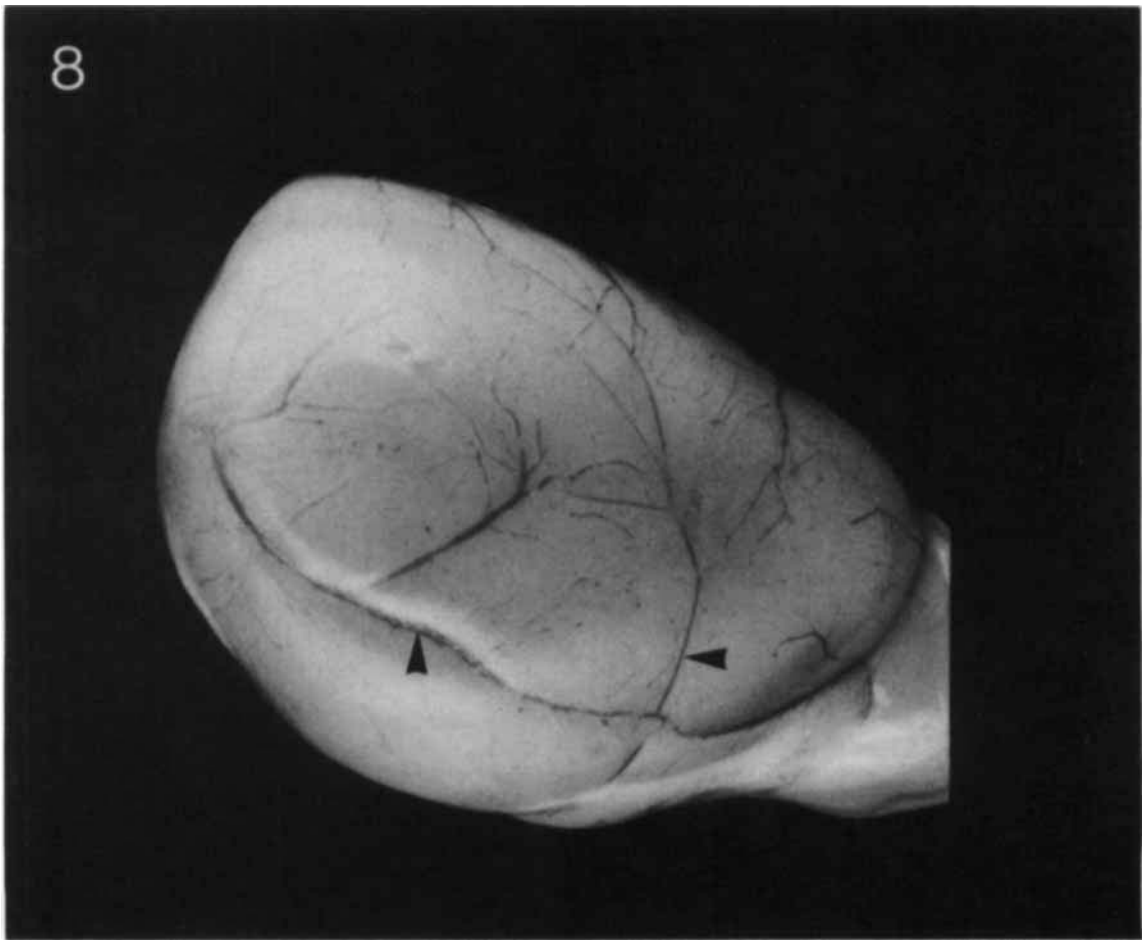

Fig. 8. The vascular pattern of the lateral surface of the rat brain. Arrows indicate two relatively invariant vascular landmarks, the middle cerebral artery (right arrow) and the inferior cerebral vein (left arrow). The inferior cerebral vein lies in the rhinal fissure. The magnification of this photograph (×7.9) was made similar to the lateral orthographic reconstruction in Figure 7. In this way the architectonic areas can be related to the vascular patterns, and measurements on both figures can be made with the scales given in Figure 7.

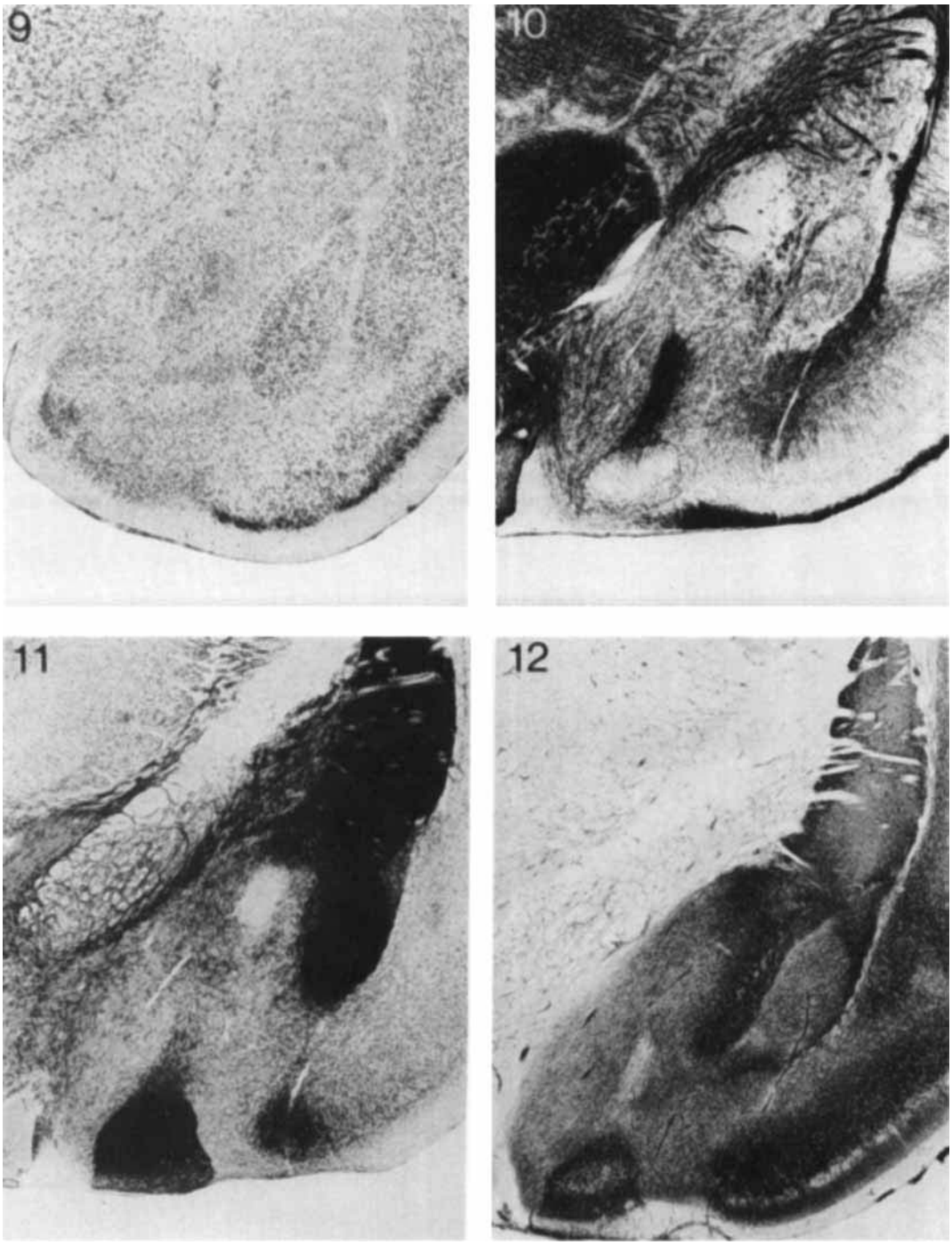

Figs. 9–12. The nuclei of the anterior one-quarter of the amygdala as they appear in sections stained for *cells* (Fig. 9), fibers (Fig. 10), AChE activity (Fig. 11), and heavy metals (Timm's method) (Fig. 12). Figures 10–12 are adjacent sections from the same brain, while Figure 9 is taken from a similar level of another brain cut at a slightly different angle. The appearance of the deep amygdaloid nuclei can be compared on all four figures, while the superficial nuclei can be compared on only Figures 10–12. See Figure 25A for designations of the different nuclei and subdivisions. ×18.2.

functionally, it is apparent that neither the primary sensory and motor cortices, nor their adjacent association cortices had connections with the amygdala. Brains with lesions that together included most of visual areas 17 and 18 (Figs. 7; 26A, #25, #17), for example, were entirely negative with respect to amygdaloid degeneration. Similarly, lesions in auditory area 41 (Figs. 7; 26B, #27), somatosensory areas 3, 40 and SII (Figs. 7; 26A,B, #19, #8, #28), primary gustatory cortex (Figs. 7; 26B, #30), and motor area 6 (Figs. 7; 26A,B, #26, #29) did not produce signs of degeneration within the amygdala. Cortical areas 14 and 40, for which functional roles cannot be assigned at present, also

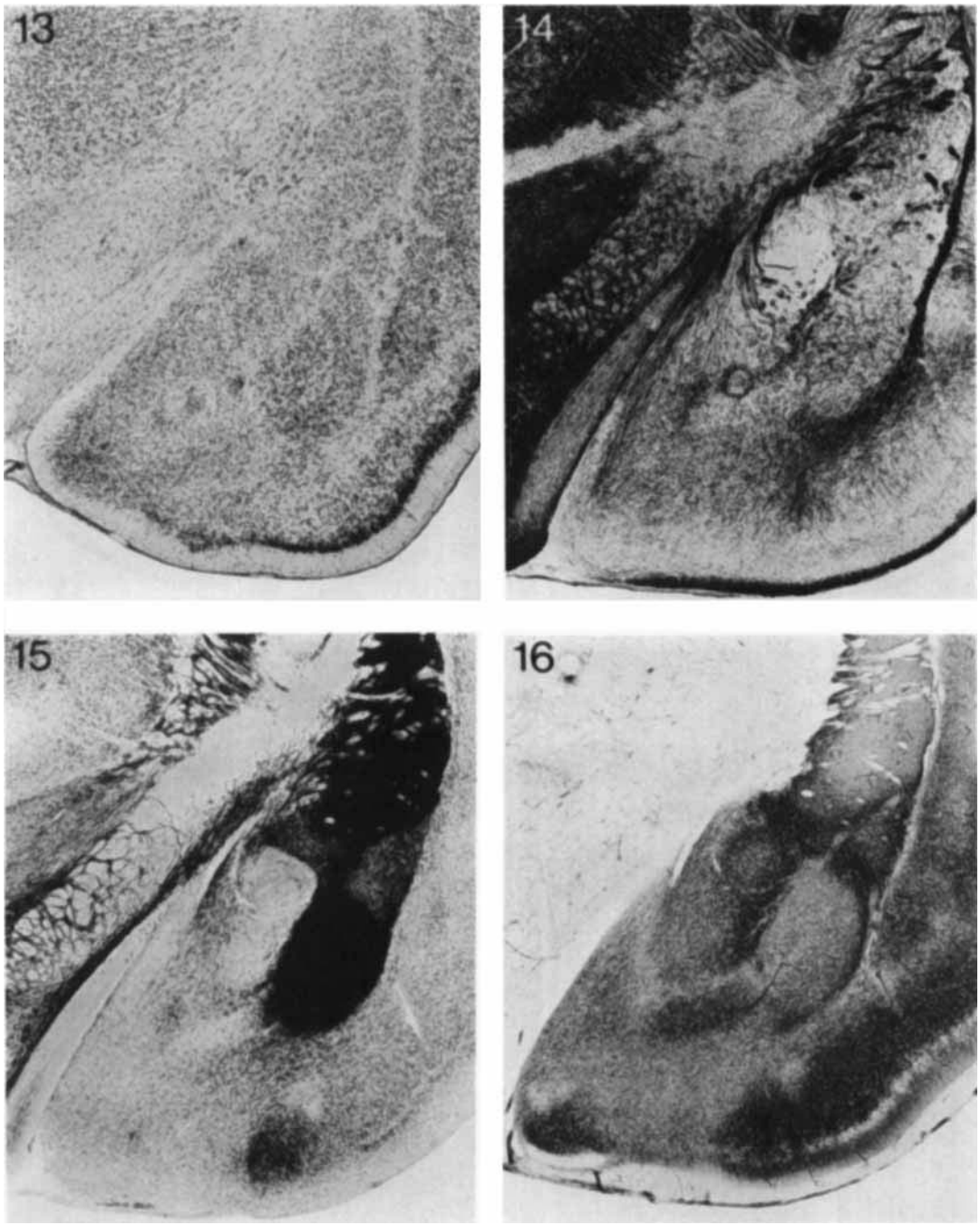

Figs. 13–16. The nuclei of the second anterior quarter of the amygdala. Stains are the same as in Figures 9–12. Figures 14–16 are adjacent sections from the same brain as in Figures 10–12, while Figure 13 is from a comparable level of another brain. See Figure 25B for designation of the different nuclei and subdivisions. ×18.2.

did not show evidence of efferents to the amygdala (Fig. 26B, #7, #8). Finally, two rats with lesions of area 35v did not yield evidence of an amygdaloid projection (Fig. 28).

Connections of lateral periallocortex with the amygdala

The periallocortex described previously lies lateral to neocortex and in contrast to it, sends efferents to the amygdala. There were nine cases of lesions that, together, included all of this cortex. Four of these, which are spaced at approximately equal intervals along the rhinal sulcus and which best illustrate the different amygdaloid termination patterns, will be discussed (Fig. 26C).

The most anterior of these lesions (Fig. 26C, #13) was approximately 1.5 mm in diameter and extended as deep as layer VI. It included the posterior parts of areas 13ad and

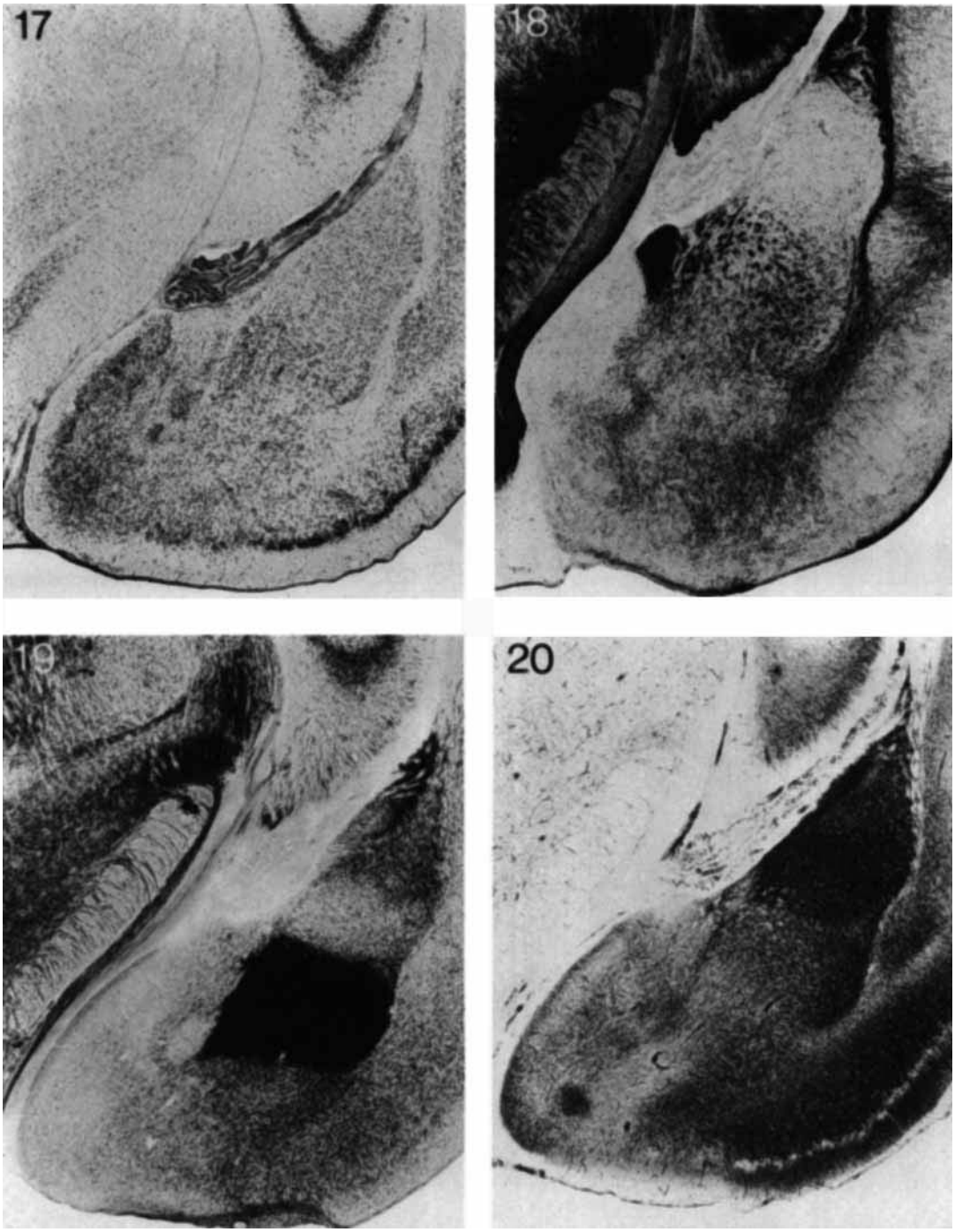

Figs. 17–20. The nuclei of the third quarter of the amygdala. The four sections shown are adjacent and from the same brain used for Figures 10–12 and 14–16. See Figure 25C for designations of the different nuclei and subdivisions. ×18.2.

13av and a small part of area 13pd. Coarse degeneration, indicative of axons, could be seen leaving the cortex, penetrating the external capsule, and entering into some of the fascicles that perforate the caudate-putamen. These fascicles could be seen to travel posteriorly. At the level of the anterior amygdala, the degenerating fibers left these bundles and fine degeneration, indicative of degenerating terminals, could be seen in several amygdaloid nuclei (Fig. 29A–D). This degeneration was densest in the anterior half of AL_2, moderate-to-heavy in the anterior portion of AL_1, AP_1, ACe, and light in AB_1.

A lesion (Fig. 26c, #14) at the posterior limit of areas 13pd and 13pv was approximately 1.8 mm in diameter in the dorsal-ventral direction, and 1.5 mm in diameter anteroposteriorly. Cortical destruction included the cells of layer VI. Coarse degeneration leaving the lesion site penetrated the

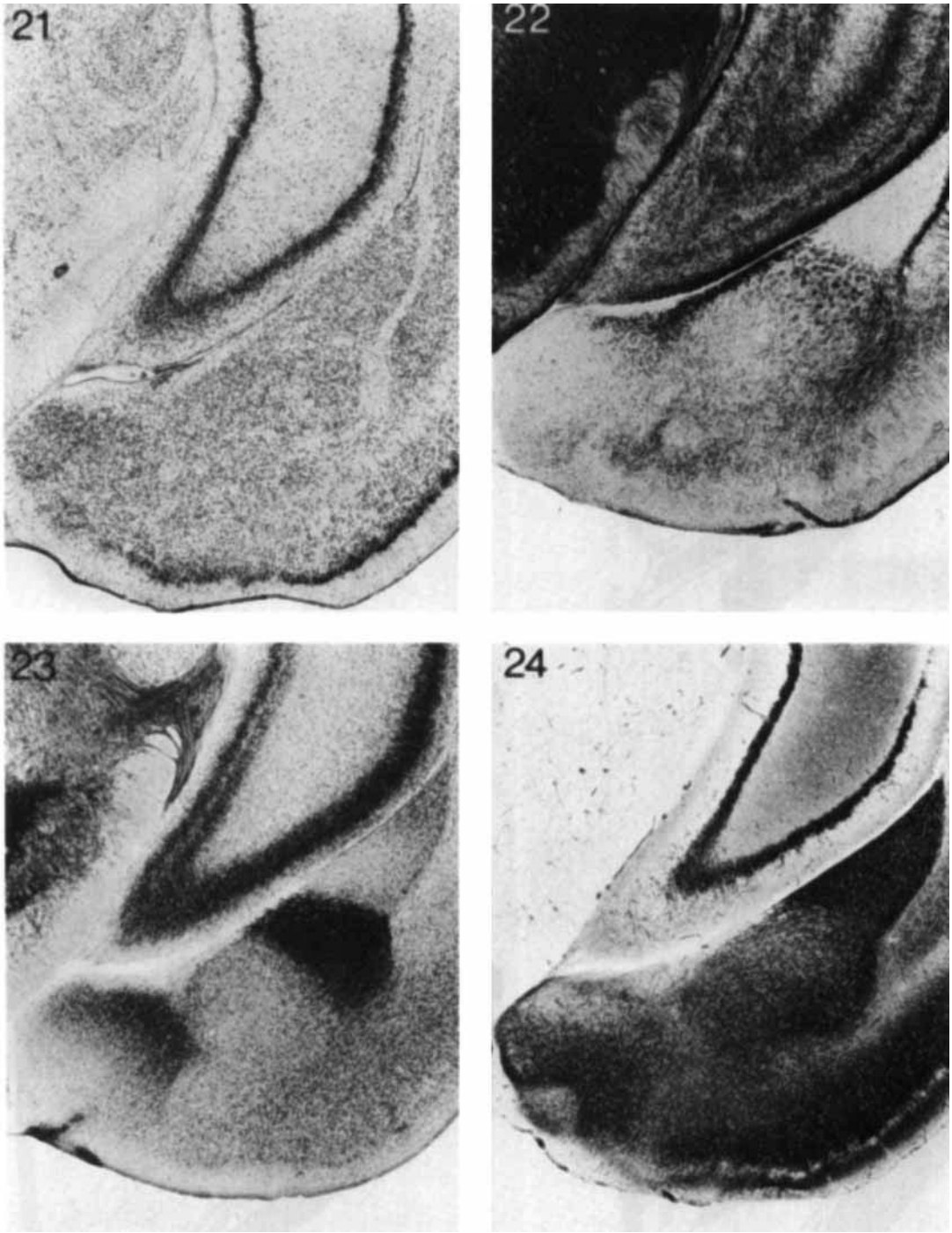

Figs. 21–24. The nuclei of the posterior one-quarter of the amygdala. The four sections shown are adjacent sections from the brain used for Figures 10–12, 14–16, and 17–20, and they are stained by the same methods. See Figure 25D for designations of the different nuclei and subdivisions. ×18.2.

external capsule and entered the caudally directed fascicles of the caudate-putamen, where they traveled for a short distance until reaching the amygdala (Fig. 29E–H). Fine, dense degeneration was observed in the anterior half of AL_1, and light degeneration was seen throughout AL_2, AP_1, and AB_1.

Further posterior, a lesion approximately 1.4mm in diameter (Fig. 26C, #16) was made in the anterior third of area 35d. In depth, the destruction extended into layer V (Fig. 27). Degenerating fibers left the lesion site and entered the external capsule, where they could be followed anteriorly until they left to terminate in the amygdala (Fig.

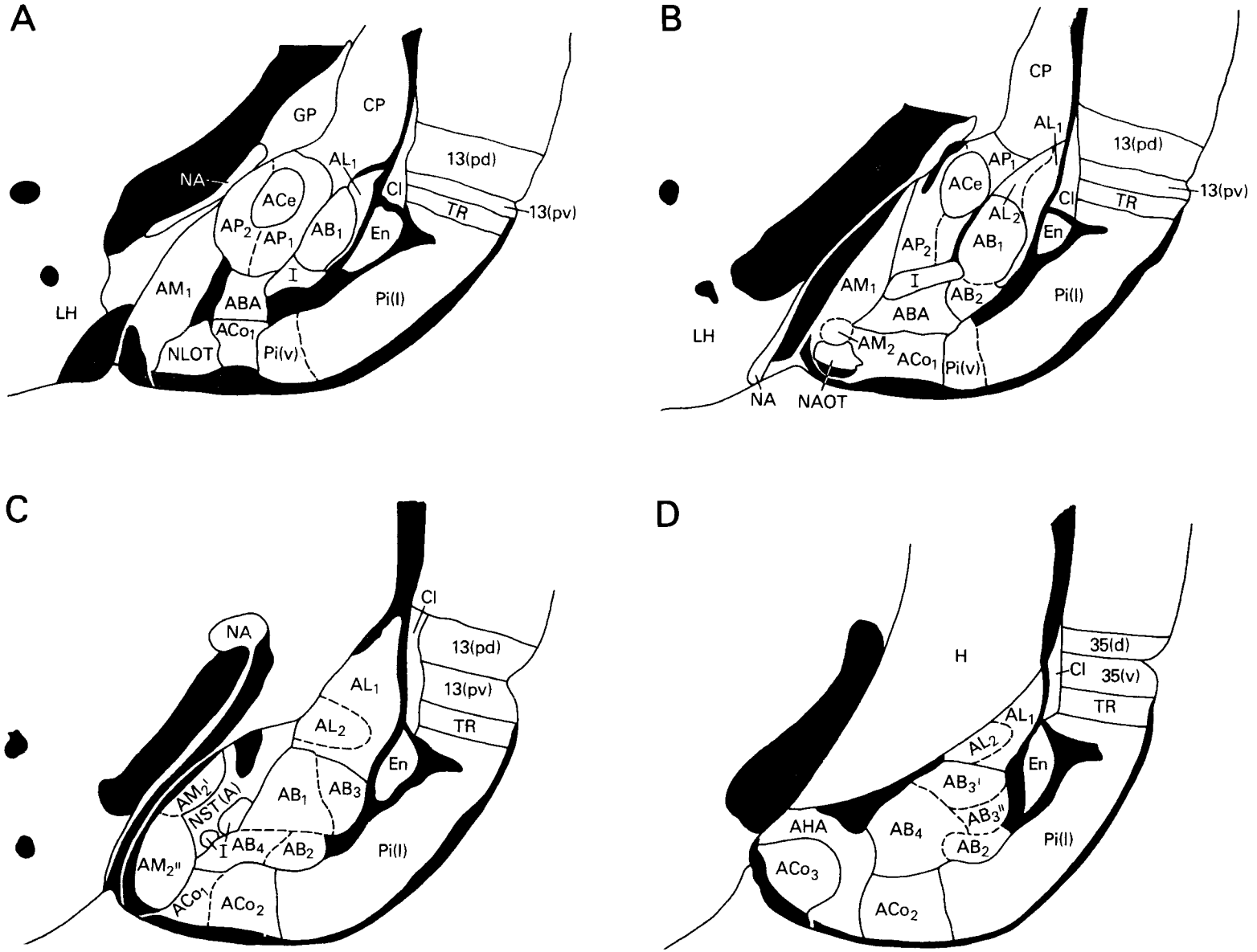

Fig. 25. Schematic drawings of the nuclear divisions of the amygdala. The different anteroposterior levels A–D were drawn from and correspond to the sections shown in Figures 10–12, 14–16, 17–20, and 21–24, respectively. Thus, each schematic drawing is based primarily on adjacent sections stained for cells, fibers, AChE activity, and heavy metals (Timm's method). For each level other closely adjacent sections from the same brain were also analyzed in order to confirm the divisions, and other brains stained by the same methods, or for catecholamine histofluorescence, were studied to insure the generality of the nuclear patterns. For legends see list of abbreviations. Fiber tracts are shown in solid black. The subdivisions on these diagrams are identical to those used in Figures 29 and 30.

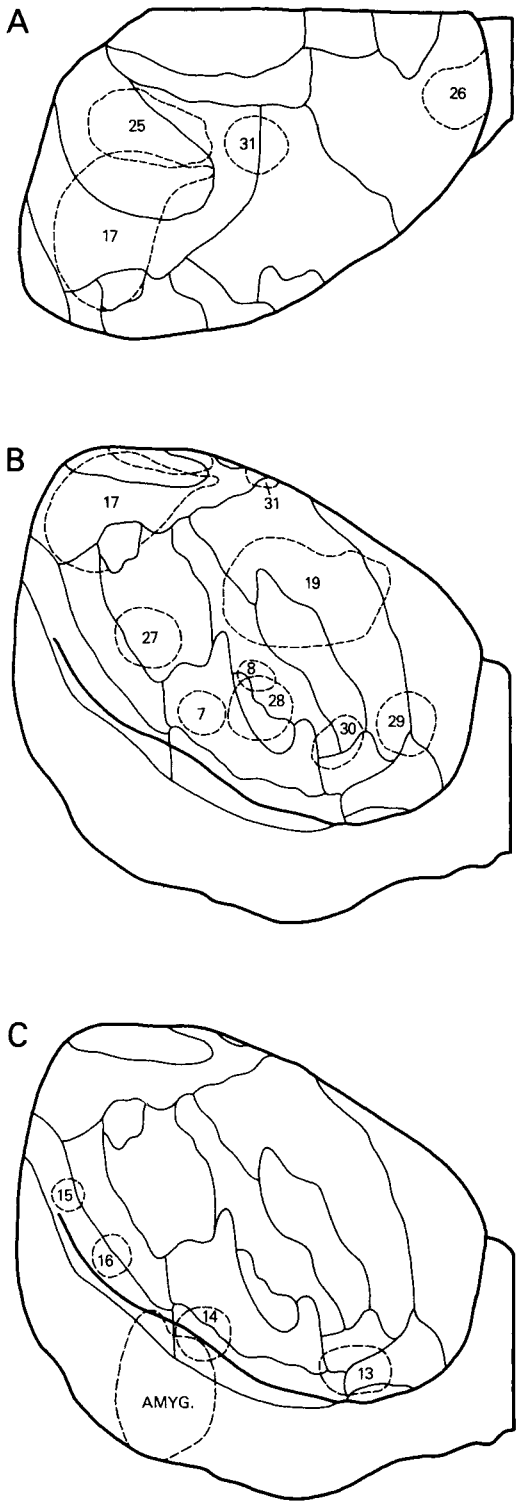

Fig. 26. Location of cortical lesions. Each lesion is marked by its case number and outlined with dashed lines. A,B. Lesions on the dorsal and the lateral surface of the brain not resulting in degeneration within the amygdala. C. Location of lesions on the lateral surface of the brain resulting in terminal degeneration in the amygdala. The location of the amygdala (AMYG.) is indicated by dashed lines.

30A–D). Degeneration of moderate density was seen in the caudal portions of AL_1 and in the posterior part of AP_1.

A lesion of about 1.3 mm in diameter was made in the caudal third of area 35d (Fig. 26C, #15). Cortical damage extended into layer V. Fiber degeneration entered the external capsule and traveled anteriorly to amygdaloid levels (Fig. 30E–H). Moderate amounts of fine degeneration were present in the posterior part of AP_1, and in all but the anterior quarter of AL_2.

DISCUSSION

Our aim in studying the cortico-amygdaloid connections of the lateral cortex in the rat was to be able to make a comparison of this system in a rodent and a primate. Homologizing a system of connections in such diverse species is risky because the degrees of phylogenetic development and types of functional specialization are so different. We will, however, now first discuss in detail the cortical and amygdaloid structures under investigation, and their interconnections, and then argue that this and other research suggest that some phylogenetic generalizations can be made about the lateral cortico-amygdaloid system.

Periallocortical architecture

Two general patterns were apparent from a histological analysis of the periallocortex. The first, which confirmed the transitional nature of the cortex, is that there is a ventral to dorsal gradient in the number of cortical laminae. For example, in Timm stains, layer II of the piriform cortex gives rise to a similar (but thicker) layer more dorsally in area 13pv, while in Nissl stains layer II (the pyramidal cell layer) of the piriform cortex gives rise in area 13pv to a layer consisting of two cell populations—a prominent layer II and a very rudimentary layer V. This II/V layer diverges dorsally in area 13pd into layers II and V, separated by a narrow layer III. Yet another layer is added still more dorsally in neocortical area 14, with a granular layer IV apparently separating off from layer III. This ventral to dorsal differentiation was neither observed in the most superficial nor the deepest layers. Thus, layer I of piriform cortex continued without change dorsally into periallocortex and neocortex, while layer III of piriform cortex gave rise to layer VI of all the more dorsal cortices. These patterns support Marin-Padilla's ('78) suggestion that layers I and VI are retained amphibian and reptilian structures which have a phylogenetic and developmental identity distinct from that of the intervening cortical layers appearing during mammalian evolution.

The second apparent pattern in the cortical histology was an anterior-posterior gradient in the just mentioned change from ventral to dorsal. In the anterior division of area 13, layer II of the piriform cortex gave rise to layers II, III, and V of area 13av. More posteriorly, the separation into these three layers was shifted dorsally to area 13pd. Finally, at the caudal third of the rhinal sulcus, this separation into three distinct layers occurred still more dorsally in area 36. In a later part of the Discussion it will be argued that anterior area 13a, the most differentiated of the lateral periallocortices, serves as an association cortex for the dorsally adjacent gustatory and lingual somatosensory neocortices. Immediately anterior to area 13a is the motor representation of the lips and tongue, and just ventral to it the olfactory-recipient piriform cortex. Thus, the motor and various sensory systems of the nasal and oropharyngeal cavities are closely related topographically in the lateral

Figs. 27,28. Cortical lesions from two cases as they appear in silver-stained sections. The lesion shown in Figure 27 (case 16) in which a portion of the upper lip of the rhinal sulcus was cauterized (see Fig. 26C), resulted in heavy amygdaloid degeneration but no hippocampal degeneration. The lesion in Figure 28, which damaged the lower lip of the rhinal sulcus, caused heavy degeneration in the lateral perforant path zone of the ipsilateral fascia dentata but not in the amygdala. ×42.

frontal, parietal and olfactory cortices. The fact that the neocortical portion of this area is the first to develop ontogenetically (Smart, '83) suggests that the functions represented here together may control the various behavioral components of suckling. From the phylogenetic point of view it has been argued that this region may have been among the first of the cortices, a telencephalic component of "an early stage in the functional transformation of the reptilian oropharyngeal apparatus" (Smart, '83). These observations lead us to propose that the development during evolution of a lactation system–a defining characteristic of mammals–necessitated the co-development of a suckling system, represented peripherally by a sensitive and plastic oropharynx and centrally by an extensive and histologically complex set of interconnected cortices that control all the sensory and motor elements of this act. These trends of early development, disproportionate representation of the oropharynx, and histological complexity of the lateral frontal and parietal cortices progress further in larger brains (Stephan et al, '81). In monkeys, for example, the anatomical homologue of this cortex (the perisylvian region, see below) is the first to develop (Sidman and Rakic, '82) and thus probably functions in suckling and later in eating. Further development of the cortical representation of the oropharynx presumably has occurred in the still larger human brain, where it organizes the sensory and motor functions of suckling, eating, and then speech.

Amygdaloid architecture

The enzyme histochemistry of the rat's amygdala provides an alternate method of arriving at a classification of the deep amygdaloid nuclei. The results clearly show that this approach confirms the major amygdaloid divisions described by previous authors on the basis of cell stains (Gurdjian, '28; Brodal, '47; Uchida, '50; Krettek and Price, '78) or AChE stains (Yu, '69). In a few instances our data verify previous suggestions (e.g., Brodal's identification of C? as the basal accessory nucleus, and Krettek and Price's redefinition of the lateral nucleus) or permit further subdivision of the nuclei (e.g., the basal nucleus). The only major reclassification concerns distinctions between the central nucleus and the overlying putamen and pallidum, for which evidence and arguments are given below.

A major problem has been to devise a nomenclature for all amygdaloid divisions that does justice to the evidence, will facilitate comparative studies, and reconciles the various designations of previous researchers. The most systematic classification of the amygdala was Brockhaus's ('38), who divided the amygdala into superficial, deep, and dorsal regions and gave the individual nuclei Latin names. This system was adapted to the rat by Uchida ('50), but it has not gained acceptance, and we, therefore, rejected this system in favor of the current usage based on topographical position. Our nuclear abbreviations reflect this (e.g., "B"

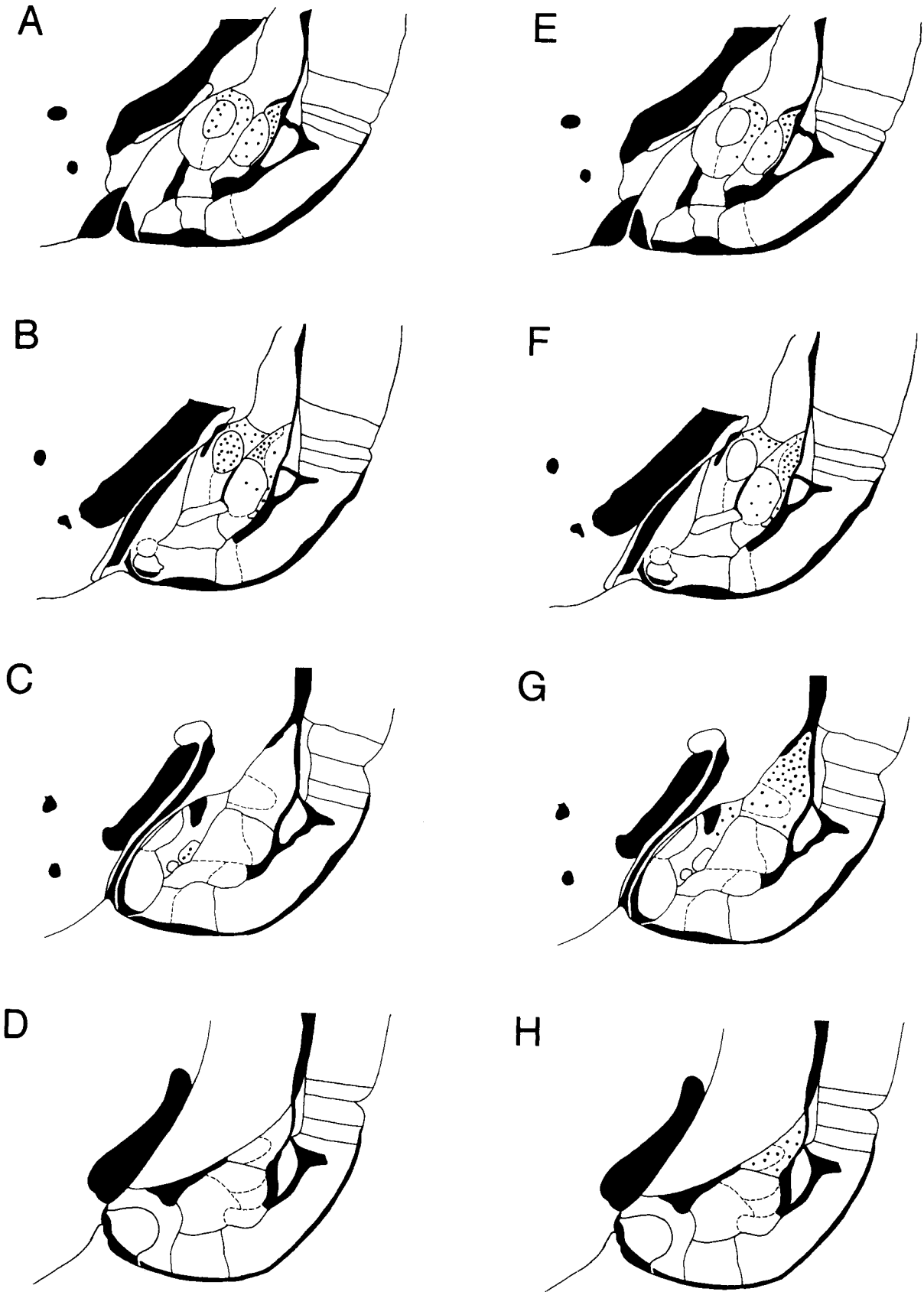

Fig. 29. Diagrams illustrating the distribution of amygdaloid afferents from rostral and caudal agranular insular cortex. Terminal degeneration has been plotted on standarized cross sections through the amygdala (see Fig. 25 for designations of specific nuclei) in order to facilitate the comparison of afferent patterns from the different cortical areas (See Figure 26C for location of lesions). A–D. The amygdaloid projections of area 13 ad (case 13). E–H. The amygdaloid projections of area 13 pd (case 14).

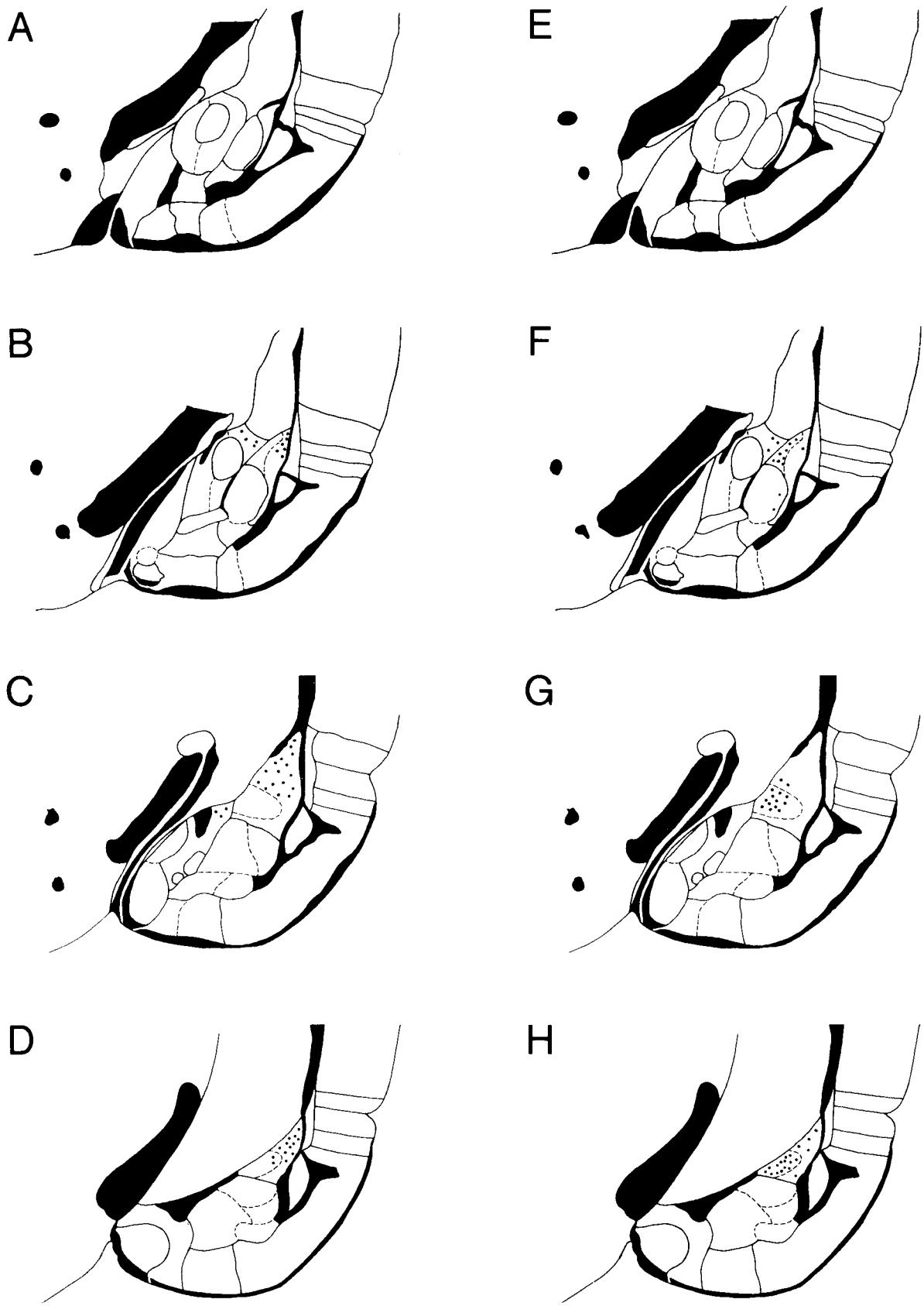

Fig. 30. Diagrams illustrating the distribution of amygdaloid afferents from rostral and caudal area 35d. Terminal degeneration has been plotted on standarized cross sections through the amygdala (See Fig. 25 for designations of specific nuclei). See Figure 26C for location of lesions. A–D. The amygdaloid projections of rostral area 35d (case 16). E–H. The amygdaloid projections of caudal area 35d (case 15).

for basal nucleus), being preceded by "A" to indicate that the nucleus is considered part of the amygdala. The use of arabic subscripts to indicate major divisions of a nucleus came from Yu ('69), while the idea of employing a prime or second mark to indicate still further subdivisions is our own.

The *lateral amygdaloid* nucleus is bounded laterally and medially by the external and intermediate capsules. Although the lateral and basal nuclei contain similar cell types (Millhouse and de Olmos, '83), the former is readily distinguished from the latter by its low AChE and fiber content. There are two divisions of this nucleus, best visible in AChE and Timm stains. They correspond to those reported by Yu ('69), and can be seen in the illustrations of Ben-Ari et al. ('77). This parcellation is further confirmed by the Golgi studies of McDonald ('84). Krettek and Price ('78) distinguished between anterior and posterior divisions of this nucleus. From their description, it would appear that these can be related to AL_1 and AL_2, respectively. We were unable to find a basis in normal material for a further separation of AL_1 and AL_2 into anterior and posterior components. However, evidence that there may be such a division emerges from the experimental data: areas 13ad and posterior 35 sent their heaviest projections, respectively, to the anterior and posterior halves of AL_2, while areas 13pd and anterior 35 send their efferents mainly to the anterior or posterior parts of AL_1.

As evidenced in the AChE and Timm stains, the *basal nucleus* is architectonically the most complex of the deep amygdaloid nuclei. Basolateral and basomedial parts have long been recognized (Brodal, '47). It is apparent from recent normal and experimental studies, however, that other subdivisions exist (Yu, '69; Krettek and Price, '78; Turner and Herkenham, '81). Our grouping of the various subdivisions under the rubric "basal" was based on topographical proximity and histochemical or cytological similarities. Nuclei AB_{1-3}, and AB_5, for example all consist of deeply stained cells, and (with the exception of AB_2) are intensely reactive for AChE. The nucleus designated AB_2 has been included in the basal rather than endopiriform category because of its proximity and similarity to AB_1 in Nissl stains and because its appearance is substantially different in AChE and Timm stains from the dorsal endopiriform nucleus. While the basomedial nucleus (AB_4) does not share the deep Nissl-and AChE-staining characteristics of these basal nuclei, it is tentatively considered as part of this group because its location and lack of AChE staining are similar to those of the basomedial nucleus in the monkey (Turner et al., '80).

An *accessory basal nucleus* is sometimes not recognized in the rat because of the difficulty of distinguishing it from the more superficial cortical nucleus (ACo_1). Nevertheless, several authors have included it in their drawings (C? of Brodal, '47; B_2 of Yu, '69) or photographs (Figs. 6, 7 of Krettek and Price, '78) of the amygdala. In our material it could be distinguished most clearly in cell stains.

As explicitly noted by Gurdjian ('28), Brodal ('47), and Krettek and Price ('78), portions of the *central nucleus* cannot be distinguished easily from several dorsally adjacent structures, the principal one of which is the putamen. A study of the rat's central amygdaloid nucleus by McDonald ('82) employing Nissl and Golgi stains addressed this problem in detail. He describes three major divisions of the central nucleus, two of which blended with overlying structures. Our histochemical material clearly confirms a tripartite division for this area (Figs. 9–12). The middle division (our ACe and McDonald's CL) is circular in shape; contains tightly packed, small round cells; is almost free of myelinated fibers; stains very lightly for AChE; appears yellow-brown in Timm staining; and contains a dense plexus of catecholamine-containing axons and axon-terminals (Fallon et al., '78), but few enkephalin-positive fibers (Haber and Nauta, '83).

This round core is surrounded medially and laterally by half-shells composed of more loosely packed cells which, as reported by McDonald, are cytoarchitectonically similar (though not identical) to the overlying putamen and adjacent structures with which they merge. The AChE histochemistry (Figs. 11, 15) and catecholamine staining (see Fig. 3C,D of Fallon et al., '78) indicate a chemical and topographic continuity with the corpus striatum, although again the staining intensities are not identical. Our AChE and Timm stains support a further distinction between medial and lateral half-shells. The same dual amygdaloid and corpus striatumlike features of these half-shells were found in stains for enkephalinlike activity (Haber and Nauta, '83): the medial half-shell appeared to be a ventral extension of the dorsal pallidum, and the lateral half-shell a ventral extension of the putamen.

We feel it is reasonable to conclude from these diverse sources of evidence that there is a region surrounding the central nucleus of the amygdala which has both amygdaloid and corpus striatumlike characteristics. We have subdivided this region into a putamenlike, lateral half (our AP_1 and McDonald's CLC) and a pallidallike, medial half (our AP_2 and McDonald's CM).

A comparison of the lateral corticoamygdaloid connections in rat and monkey

The problems involved in classifying the divisions of the cortex lying along the rhinal sulcus in the rat have been discussed by Guldin and Markowitsch ('83). Based on their experiments of thalamic afferents, these authors designate as "insular" the cortex lining the entire length of the rhinal sulcus, with prefrontal, gustatory (somatosensory) and associative subdivisions.

The "prefrontal" division generally corresponds to the dorsal and ventral agranular insula of Krettek and Price ('77a) and our areas 13ad and 13av. We suggest that this cortex is a gustatory/lingual somatosensory association area, since its cortical afferent supply is probably from the adjacent gustatory/lingual ("G" in Fig. 7) cortex (Turner and Zimmer, '80; Norgren and Wolf, '75; Turner, '81). Its amygdaloid projections (Figs. 26C, #13; 29A–D) are to ACe, AB_1, AP_1, and anterior AL_2 (Turner and Zimmer, '80; Veening, '78; Ottersen, '82). The analogous cortex in the monkey is the agranular and anterior dysgranular insula. In this species also its afferents are probably from the dorsally adjacent "G" (Jones and Burton, '76; Morse et al., '80), and its efferents are to ACe, medial AB, ventral putamen, and dorsomedial AL (Turner et al., '80).

The "gustatory (somatosensory)" cortex of Guldin and Markowitsch generally corresponds to the posterior, agranular insula of Krettek and Price ('77a) and our areas 13pd and 13pv. This cortex receives afferents from the somatosensory cortices SI and SII (Turner and Zimmer, '80; Turner, '81) and from visceral relays in the brainstem (Saper, '82). We therefore suggest that this is an association cortex of both visceral and cutaneous modalities of the somatosensory system. The amygdaloid projections of this cortex in

the rat (Figs. 26C, #14; 29E–H) are to AL_1, AB_1, and AP_1. In the monkey, the analogous cortex is the granular and posterior dysgranular insula, which receives afferents from the overlying SII (Friedman, '83). The granular insula in this species projects to dorsomedial AL, and the dysgranular insula projects to both dorsomedial AL and to AB (Turner et al., '80; Mufson et al., '81).

Finally, the "associative insular" cortex of Guldin and Markowitsch corresponds generally to the perirhinal cortex of Krettek and Price ('77a) and to our areas 35d and 35v. In the rat, this amygdalopetal cortex and a strip lying above it (area 36) receive afferents from, respectively, the visual and auditory association cortices (Turner and Zimmer, '80 Turner, '81). This suggests that area 35 in the rodent may correspond to the amygdalopetal visual area 20 in the carnivore (Heath and Jones, '71) and to amygdalopetal visual areas 20, 21, and ventral 38 in the primate. Area 36 in the rodent may correspond to the ventral amygdalopetal auditory cortex in the carnivore (Russchen, '82) and to amygdalopetal auditory areas 22 and dorsal 38 in the primate (Turner et al., '80). If this analogy is correct both "perirhinal" and the Brodmann numbers do not designate homologous structures in the two species. We hypothesize that area 35d and possibly the far posterior part of 13pd (Hughes, '77) is a temporal visual association area in the rat. It projects to caudal AL_2 (Figs. 26C, #15; 30E,F; Turner and Zimmer, '80; Veening, '78; Ottersen, '82), and the analogous cortices in the monkey project to AL, AB, and ABA (Turner et al., '80). We also suggest that area 36 in the rodent is temporal auditory association cortex. Our lesion (Fig. 26C, #16) straddled the boundary line of anterior 36 and 35d, and projected to caudal AL_1. The analogous cortex in the monkey projects to AL, AB, and ABA (Turner et al., '80; Herzog and Van Hoesen, '76).

From these limited comparative data, several phylogenetic generalizations (which should serve at present only as hypotheses to be tested!) may be made about the place and role of lateral amygdalopetal cortex in the mammalian cerebrum.[1] In rodents, this cortex is periallocortical in type and is located along the length of the rhinal sulcus. A shallow, convex deflection of the sulcus occurs at the boundary between the insular and temporal cortices (see Figs. 7, 8, left arrowhead), and marks the location of what will become a major branch of this sulcus-the Sylvian fissure. In carnivores, the insular cortex at this junction invaginates to form the pseudo-Sylvian sulcus and therefore the beginning of a temporal lobe and an "island." Most of the amygdaloid-projecting cortex in the cat is periallocortical, but there is apparently a small temporal neocortical component (Russchen, '82). Finally, in the rhesus monkey, continued development of the insular and temporal cortices results in the complete separation of the rhinal and Sylvian sulci; topographically distinct temporal lobes and insulae; and the formation within the latter of the circular sulcus. In this species neocortical efferents to the amygdala appear more extensive than the periallocortical ones. Amygdalopetal cortex begins dorsally with the agranular and dysgranular insula and extends without interruption over the surface and sulci of the neocortex forming the temporal lobes, ending medially in the rhinal sulcus. Thus it appears that it is the phylogenetic elaboration of the amygdaloid-projecting lateral periallocortex and the posterior movement and invagination of its anterior half that results in the formation of the amygdaloid-projecting anterior insula and temporal lobes of primates.

In the species studied this lateral amygdalopetal cortex appears to consist of four functional divisions, which phylogenetically maintain their topographical positions with respect to each other. The first two are located in the insula, the second two in the temporal lobe: (1) anterior, agranular insula in all species studied; (2) posterior, agranular insula in rodents and carnivores, and granular and posterior dysgranular insula in primates; (3) area 36 in rodents, areas 36 and ventral 22 in carnivores, and anterior area 22 and dorsal area 38 in primates; and (4) area 35 in rodents, area 20 in carnivores, and anterior areas 20, 21, and ventral 38 in primates. Interhemispheric connections of all these cortices are by way of the anterior commissure in both rat (Horel and Stelzner, '81) and monkey (Turner et al., unpublished observations). Functionally, these four divisions appear to be modality-specific regions which belong, respectively, to (1) gustatory (and possibly lingual somatosensory), (2) somatosensory (including visceral), (3) auditory, and (4) visual systems. The functional identity of each of these four divisions derives from modality-specific cortical relays that ultimately originate in one of the four primary sensory areas of the neocortex. These non-amygdalopetal cortical relays are interhemispherically connected by the corpus callosum (Pandya et al., '71). The present analysis of cortico-amygdaloid termination patterns in the rat extend those made in the monkey (Turner et al., '80) in demonstrating that the components of the four neocortical sensory systems that are destined to affect limbic functions maintain their anatomical (and probably functional) identity at least as far as the amygdaloid complex (Turner, '81). A final set of relays may compose the connections that each of the amygdaloid nuclei makes with the autonomic and endocrine nuclei of the brain.

ACKNOWLEDGMENTS

This research was supported by NIH grant MH 25495 and Aarhus University. Additional salary support for the first author was provided by Aarhus University. The authors are grateful for the expert assistance of K. Christensen, D. Jensen, M. Knapp, I. Larsen, A. Meier, L. Munkoe, Th. Nielsen, M. Sorenson, E. Traerup, and K. Wiedemann.

We profited from the help of Dr. Anders Bjorklund in the preparation of the histofluorescent material, and from our discussions with Dr. Jose de Olmos concerning amygdaloid anatomy.

[1]These generalizations may also apply to avians and reptiles, but at present anatomical homologies between submammals and mammals cannot be made with certainty. See Northcutt ('81).

LITERATURE CITED

Ben-Ari, Y., R.E. Zigmond, C.C.D. Shute, and P.R. Lewis (1977) Regional distribution of choline acetyltransferase and acetylcholinesterase within the amygdaloid complex and stria terminalis system. Brain Res. *120*:435–445.

Brockhaus, H. (1938) Zur normalen und pathologischen Anatomie des Mandelkerngebietes. J. Psychol. *49*:1–148.

Brodal, A. (1947) The amygdaloid nucleus in the rat. J. Comp. Neurol. *87*:1–16.

Fallon, J.H., D.A. Koziell, and R.Y. Moore (1978) Catecholamine innervation of the basal forebrain. III. Amygdala, suprarhinal cortex and entorhinal cortex. J. Comp. Neurol. *180*:509–532.

Fink, R., and L. Heimer (1967) Two methods for selective silver impregnation of degenerating axons and their synaptic endings in the central nervous system. Brain Res. *4*:369–374.

Friedman, D.P. (1983) Laminar patterns of termination of cortico-cortical afferents in the somatosensory system. Brain Res. *273:*147–151.

Geneser-Jensen, F., and Th.W. Blackstad (1971) Distribution of acetylcholinesterase in the hippooampal region of the guinea pig. Z. Zellforsch. *114:*460–481.

Guldin, W.O., and H.J. Markowitsch (1983) Cortical and thalamic afferent connections of the insular and adjacent cortex of the rat. J. Comp. Neurol. *215:*135–153.

Gurdjian, E.A. (1928) The corpus striatum of the rat. Studies on the brain of the rat, no. 3. J. Comp. Neurol. *45:*249–281.

Haber, S.N., and W.J.H. Nauta (1983) Ramifications of the globus pallidus in the rat as indicated by patterns of immunohistochemistry. Neuroscience. *9:*245–260.

Hall, E., and F. Geneser-Jensen (1971) Distribution of acetylcholinesterase and monoamine oxidase in the amygdala of the guinea pig. Z. Zellforsch. *120:*204–221.

Haug, F.M. (1973) Heavy metals in the brain. A light microscope study of the rat with Timm's sulphide silver method.. Methodological considerations and cytological and regional staining patterns. Adv. Anat. Embryol. Cell Biol. *47:*1–71.

Heath, C., and E. Jones (1971) Anatomical organization of the suprasylvian gyrus of the cat. Ergebn. Entw. Gesch. *45:*1–64.

Herzog, A.G., and G.W. Van Hoesen (1976) Temporal neocortical afferent connections to the amygdala in the rhesus monkey. Brain Res *115:*57–69.

Hess, D.T., and B.H. Merker (1983) Technical modifications of Gallyas' silver stain for myelin. J. Neurosci. Methods *8:*95–97.

Hjorth-Simonsen, A. (1970) Fink-Heimer silver impregnation of degeneration axons and terminals in mounted cryostat sections of fresh and fixed brains. Stain Technol. *45:*199–204.

Horel, J.A., and D.J. Stelzner (1981) Neocortical projections of the rat anterior commissure. Brain Res. *220:*1–12.

Hughes, H.C. (1977) Anatomical and neurobehavioral investigations concerning the thalamo-cortical organization of the rat's visual system. J. Comp. Neurol. *175:*311–335.

Jones, E.G., and H. Burton (1976) Areal differences in the laminar distribution of thalamic afferents in cortical fields of the insular, parietal, and temporal regions of primates. J. Comp. Neurol. *168:*197–248.

Krettek, J.E., and J.L. Price (1978) A description of the amygdaloid complex in rat and cat, with observations on intra-amygdaloid axonal connections. J. Comp. Neurol. *178:*255–280.

Krieg, W.J.S. (1946) Connections of the cerebral cortex. I. The albino rat. A. Topography of the cortical areas. J. Comp. Neurol. *84:*221–276.

Loren, I., A. Bjorklund, B. Falck, and O. Lindvall (1980) The aluminum-formaldehyde (alfa) histofluorescence method for improved method for improved visualization of catecholamines and indoleamines. 1. A detailed account of methodology for central nervous tissue using paraffin, cryostat or vibratome sections. J. Neurosci. Methods. *2:*277-300.

Marin-Padilla, M. (1978) Dual origin of the mammalian neocortex and evolution of the cortical plate. Anatomy and Embryology. *152:*109–126.

McDonald, A.J. (1982) Cytoarchitecture of the central amygdaloid nucleus of the rat. J. Comp. Neurol. *208:*401–418.

McDonald, A.J. (1984) Neuronal organization of the lateral and basolateral amygdaloid nuclei in the rat. J. Comp. Neurol. *222:*589–606.

Millhouse, O.E., and J. de Olmos (1983) Neuronal configurations in lateral and basolateral amygdala. Neuroscience, *10:*1269–1300.

Morse, J.R., and R.M. Beckstead, T. Pritchard, and R. Norgren (1980) Ascending gustatory and visceral afferent pathways in the monkey. Soc. Neurosci. Abstr. *6:*307.

Mufson, E.J., M.M. Mesulam, and D.N. Pandya (1981) Insular interconnections with the amygdala in the rhesus monkey. Neuroscience. *6:*1231–1248.

Norgren, R., and G. Wolf (1975) Projections of thalamic gustatory and lingual areas in the rat. Brain Res. *92:*123–129.

Northcutt, R.G. (1981) Evolution of the telencephalon of nonmammals. In W.M. Cowan, Z.W. Hall, and E.R. Kandel (eds): Annual Review of Neuroscience. *4:*301–350.

Olmos, J.S., S.V.O. Ebbesson, L. Heimer, and M.J. Robards (eds) (1981) Neuroanatomical Tract-Tracing Methods. New York: Plenum, pp. 117–170.

Ottersen, O.P. (1982) Connections of the amygdala of the rat. IV. Corticoamygdaloid and intraamygdaloid connection as studied with axonal transport of horseradish peroxidase. J. Comp. Neurol. *205:*30–48.

Pandya, D.N., E.A. Karol, and D. Heilbronn (1971) The topographical distribution of interhemispheric projections in the corpus collosum of the rhesus monkey. Brain Res. *32:*31–43.

Russchen, F.T. (1982) Amygdalopetal projections in the cat. I. Cortical afferent connections. A study with retrograde and anterograde tracing techniques. J. Comp. Neurol. *206:*159–179.

Saper, C.B. (1982) Convergence of autonomic and limbic connections in the insular cortex of the rat. J. Comp. Neurol. *210:*163–173.

Sidman, R.L., and P. Rakic (1982) Development of the human central nervous system. In: Histology and Histopathology of the Nervous System. W. Haymaker and R. Adams, eds. Thomas, Springfield, pp. 3–145.

Smart, I.H.M. (1983) Three dimensional growth of the mouse isocortex. J. Anat. *137:*683–694.

Stephan, H., H. Frahm, and G. Baron (1981) New and revised data on volumes of brain structures in insectivores and primates. Folia Primatol. *35:*1–29.

Tanaka, D., Jr. (1976) Thalamic projections of the dorsomedial prefrontal cortex in the rhesus monkey (Macaca mulatta). Brain Res. *110:*21–38.

Turner, B.H., and M. Herkenham (1981) An autoradiographic study of thalamoamygdaloid connections in the rat. Anat. Rec. *199:*260A.

Turner, B.H., and J. Zimmer (1980) Connections between the cerebral cortex and amygdala in the rat. Soc. Neurosci. Abstr. *6:*113.

Turner, B.H., M. Mishkin, and M. Knapp (1980) Organization of the amygdalopetal projections from modality-specific cortical association areas in the monkey. J. Comp. Neurol. *191:*515–543.

Uchida, Y. (1950) A contribution to the comparative anatomy of the amygdaloid nuclei in mammals, especially in rodents. I. Rat and mouse. Folia Psychiatr. Neurol. Jpn. *4:*25–42.

Veening, J.E. (1978) Cortical afferents of the amygdaloid complex in the rat: an HRP study. Neurosci. Lett. *8:*191–195.

Yu, H.H. (1969) The amygdaloid complex in the rat. Ph.D. dissertation, University of Ottawa, pp. 1–83.